

Analysis of CMIP6 Simulations in the Indian Summer Monsoon Period 1979-2014

Lakshmana Rao Vennapu^{1†}, Krishna Dora Babu Kotti², Sravani Alanka³ and Pavan Krishnudu Badireddi⁴

¹Department of Meteorology and Oceanography, Andhra University, Visakhapatnam, India

²Department of Geography, School of Distance Education, Andhra University, Visakhapatnam, India

³Flood Meteorological Office, Meteorological Center Hyderabad, IMD, India

⁴Ideal Institute of Technology, Kakinada, East Godavari, India

†Corresponding author: Lakshmana Rao Vennapu; lakshman.met@gmail.com

Key Words	Global climate, Coupled model, Climate change
DOI	https://doi.org/10.46488/NEPT.2024.v24i01.B4215 (DOI will be active only after the final publication of the paper)
Citation of the Paper	Lakshmana Rao Vennapu, Krishna Dora Babu Kotti, Sravani Alanka and Pavan Krishnudu Badireddi, 2025. Analysis of CMIP6 Simulations in the Indian Summer Monsoon Period 1979-2014. <i>Nature Environment and Pollution Technology</i> , Vol. 24, No. 1, B44215. https://doi.org/10.46488/NEPT.2024.v24i01.B4215

ABSTRACT

The monsoon system in India plays a pivotal role in shaping the country's climate. Recent studies have indicated that the increasing variability of monsoons is attributable to climate change, resulting in prolonged periods of drought and excessive rainfall. Understanding, analyzing, and forecasting monsoons is crucial for socioeconomic sustainability and communities' overall well-being. Climate forecasts, which project future Earth climates typically up to 2100, rely on models such as the Couple Model Intercomparison Project (CMIP). However, confidence in these forecasts remains low due to the limitations of global climate models, particularly in terms of capturing the intricacies of monsoon dynamics, notably from June to September. To address this issue, researchers have examined precipitation simulations under various future scenarios using both CMIP5 and the latest CMIP6 models. Evaluating the performance of these models from 1979 to 2014, particularly in simulating mean precipitation and temperature, has revealed improvements in multi-model ensembles (MME), highlighting advancements in monsoon characteristics. By comparing the CMIP5 and CMIP6 models, researchers have identified the most reliable models for climate downscaling research, which can provide more accurate predictions of regional climate changes, thereby offering valuable insights for enhancing climate modeling in the Indian subcontinent.

INTRODUCTION

Over the previous century, there have been notable alterations in the temporal and spatial distributions of worldwide precipitation, increasing both the frequency and intensity of natural calamities (Zhang et al. 2016). Human actions, such as the emission of greenhouse gases and modifications in land usage, have brought about a 1°C elevation in the global mean temperature

since the pre-industrial era, inducing extreme weather, oceanic warming, acidification, and modifications in ecosystems, which are anticipated to endure throughout the 21st century. The mean global surface temperature grew by 0.99°C from 1850 to 1900 during the initial two decades of the 21st century (IPCC Report 2021). Alterations in land use and land cover (LULC) affect the physical characteristics of the Earth's surface, thereby regulating the transfer of moisture, kinetic energy, and heat into the atmosphere, consequently influencing localized or regional variations in surface temperatures (Bonan 2008).

India's economy is heavily dependent on the agricultural sector, where the Southwest Monsoon season contributes to 75% of its total rainfall. Fluctuations in monsoon precipitation have a significant impact on various aspects, such as agriculture, the economy, water availability, power production, and ecosystems. Analyzing these variations is crucial for minimizing negative consequences and anticipating droughts and floods. Alterations in global climate patterns and rising global temperatures could influence the circulation of monsoons. Krishnan (2012) examined the response of the South Asian monsoon (SAM) system to global climate change. Their findings revealed a decline in the strength of the overturning boreal summer monsoon circulation and the southwesterly monsoon flow over the last five decades. This decline has been linked to a reduction in the number of days with moderate-to-heavy monsoon rainfall and upward vertical air movements. If this trend continues, it is projected that by the conclusion of the 21st century, there will be a diminished large-scale monsoon flow, weaker vertical air velocities will weaken, and orographic precipitation in the Western Ghats Mountains will decrease.

The unpredictability and irregularity of monsoons have led to substantial financial losses, damage to individuals and assets, and devastation of agricultural areas and the ecosystem in recent years, prompting concerns regarding food insecurity. Consequently, the prediction and comprehension of monsoon rainfall patterns have emerged as focal points for many Asian nations (Reuter et al. 2013).

Observations of the Indian summer monsoon in central India have revealed a declining trend in rainfall during the latter half of the 20th century (Ramanathan et al. 2005, Bollasina et al. 2011, Mishra et al. 2012, 2014, Jin & Wang 2017). The diminishing pattern of the Indian monsoon is linked to greenhouse gas-induced warming of the sea surface of the Indian Ocean, while simultaneous warming across the Indian subcontinent has been mitigated by aerosols and alterations in land cover (Deser et al. 2010).

Recent studies utilizing global coupled models generally agree that the Indian monsoon precipitation is projected to rise as a result of climate change throughout the 21st century (Chaturvedi et al. 2012, Menon et al. 2013, Lee & Wang 2014, Asharaf & Ahrens 2015, Mei et al. 2015, Sharmila et al. 2015). The sixth phase of the Coupled Model Intercomparison Project (CMIP6) has introduced enhanced global climate models (GCMs) that aim to overcome the limitations of CMIP5 by incorporating advanced physical algorithms. These updated models now incorporate "Shared Socioeconomic Pathways" (SSPs), aligning future radiative forcing scenarios with socioeconomic storylines (Song et al. 2020, Si et al. 2020). It is crucial to comprehend the advantages of the CMIP6 model over the CMIP5 model and assess their

accuracy before using their climate predictions in decision-making and policy formulation. In the present work, we evaluate the performance of two generations of climate models, CMIP5 and CMIP6, by comparing their ability to simulate mean precipitation and temperature over the historical period from 1979 to 2014.

Our objective was also to analyze the improvements in the multi-model ensemble (MME) from CMIP6 for monsoon characteristics. Spatial and temporal, we studied the mean precipitation changes interannual and spatially in both generations of the models (CMIP 5 and CMIP 6). This study aimed to assess the enhancements in the CMIP6 MME of monsoon characteristics, focusing on mean precipitation. Apart from this, the study compares projections from seven CMIP5 models and eight CMIP6 models for various atmospheric parameters, such as precipitation, winds, and pressure, especially during the 36-year Southwest Monsoon period over 36 years (1979-2014), both spatially and temporally. Various statistical skill scores, such as Taylor and interannual variability scores, were used for both temporal and spatial analyses of the atmospheric parameters. We specifically compared the ensemble model mean precipitation patterns with the IMD-observed precipitation in the past and present. The major objective of this study was to evaluate the valuation of the performance of two generations of climate models: CMIP5 and CMIP6. For all models in the two generations, mean precipitation overestimated the observed interannual spatial variance.

DATA AND METHODOLOGY

In the present study, the monthly data of 7 CMIP5 and 8 CMIP6 models were taken for a period of 36 years from 1979 to 2014 with a horizontal resolution of $2.50^{\circ} \times 2.50^{\circ}$. For validation of the model simulations, the IMD gridded data were used for evaluation of atmospheric variables temperature and precipitation, while ECMWF reanalysis datasets were used to evaluate the Mean Sea Level Pressure (MSLP) and winds at 850 hPa. Gridded climate data for temperature and precipitation (Pai et al. 2014) is obtained from the India Meteorological Department (IMD). Gridded precipitation dataset from IMD is available at a much finer spatial resolution, i.e., $0.25^{\circ} \times 0.25^{\circ}$ (Pai et al. 2014) for the period 1979-2014 are used for analysis. Precipitation data from Pai et al. 2014 is used for mapping observed precipitation bias over India for the period 1979-2014. IMD provides gridded temperature data at a resolution of $1^{\circ} \times 1^{\circ}$ for the period 1951 to 2019. Recently, IMD has also introduced a new temperature data product at $0.5^{\circ} \times 0.5^{\circ}$ resolution for the limited period of 1980-2019, which roughly translates into 50 Km in length and 50 km in width (Srivastava et al. 2009), which is used for observation.

ERA5 is the fifth generation of ECMWF atmospheric reanalysis of the global climate. ERA5 Climate reanalysis gives a numerical description of the recent climate, produced by combining models with observations. ERA5 combines vast amounts of historical observations into global estimates using advanced modeling and data assimilation systems. ERA-Interim (Dee et al. 2011) monthly datasets are used for pressure at mean sea level and meridional and zonal winds during the June-September period of 1979-2014 with a spatial resolution of 1×1 . CMIP-5 models and CMIP-6 models used for the study are shown in Tables 1 and 2, respectively.

MATERIALS AND METHODS

We used the Taylor diagram metric (Taylor 2001) to assess the overall performance of each model against the observational performance. Bias correction and panel plotting were performed to compare the model and observations. These were performed using GRADS and FERRET software. Recently, many studies have demonstrated that the Taylor diagram can be used to summarize the relative merits of a collection of different models (Taylor 2001). This study also estimated the required statistical scores for the observed and model data and displayed them using a Taylor diagram. This shows the relative skill of test fields simulated by different models to match the observation in terms of correlation, standard deviation, and centered root-mean-square differences. Ranking CMIP6 models based on their performance in simulating multiple variables over different timeframes is a challenging task because a GCM may show various degrees of accuracy for different variables and timeframes. Taylor Score, root mean square error, and interannual variability scores in the spatial domain are estimated and displayed in bar diagrams.

RESULTS AND DISCUSSION

Several studies have highlighted the shortcomings of CMIP5 models in consistently overestimating or underestimating monsoon characteristics over South Asia and the Indian subcontinent, depending on different precipitation indices. This inconsistency reduces confidence in future projections. Over the past decade, various statistical and dynamic downscaling approaches (Kannan & Ghosh 2013, Salvi 2013) have been proposed to improve local-scale simulations. However, these approaches have not consistently resulted in significant improvements and sometimes even worse results (Sharma 2018).

Comparative Evaluation of Temperature in the CMIP5 and CMIP6 Models

Fig. 1 shows a Taylor diagram illustrating the ability of global climate models to simulate monthly mean precipitation during the Indian summer monsoon. Eight models were analyzed, with the blue contours representing the root mean square error and the radial distance from the origin representing the standard deviation. Models close to the observation point have high correlation and low RMS errors, whereas models directly at the observation point have the correct standard deviation.

All models overestimated the observed interannual spatial variance. The temperatures of GISS-E2.1-G (CMIP6), GISS-E2-R (CMIP5), and CESM-1 (CMIP5) were very close to the observations, whereas all other models were far from the observation values. Ensembles of both CMIP5 and CMIP6 models showed a high correlation with observations, which is a good representation for modeling. The Taylor Score shows the relative performance of the model. The score is relatively skillful and simulates both the amplitude and pattern of variability (RMSE and Correlation).

From Fig. 2 and Table 3, the Taylor score of GISS-E2.1-G, HAD-GEM-GC3.1, MPI-ESM-1.2 of the CMIP6 models, and ACCESS-CM1 and CESM1 of the CMIP5 models have the highest skill scores, while the other models have low skill scores. A key measure of a climate model's effectiveness is its ability to realistically simulate interannual variability.

The Interannual Variability Skill (IVS) metric is used to evaluate this performance. A smaller IVS value indicates that the model is better at capturing interannual variability.

In Fig. 3, the IVS for GISS-E2.1-G of the CMIP6 and GISS-E2-R models and the CESM1 of the CMIP5 models show the highest skill (low values) compared to the other models.

Comparative Evaluation of Precipitation in the CMIP5 and CMIP6 Models

In Fig. 4 and Table 4, the CMIP5 and CMIP6 models show low correlation values for precipitation compared to the temperatures (Fig. 1). Of all the models, the GISS-E2.1-G, CESM-2 of the CMIP6, and MIROC5 of the CMIP5 model simulations are coming closer to the observations, which indicates better performance compared to the other models.

In Fig. 5, the Taylor scores of ACCESS-CM-1, MIROC5 of CMIP5, and GISS-E2.1-G of the CMIP6 models are shown as having the highest skill (high values), while the rest of the models have low skill (low values). In Fig. 6, the Interannual Variability Score of MIROC5 of the CMIP5 models and GISS-E2.1-G CESM-2 of the CMIP6 models show high IVS skill scores (low values) compared with the rest of the models.

Evaluation of the CMIP6 Model Skill During the Indian Summer Monsoon

Evaluation of temperature in CMIP6 models: Fig. 7 shows the spatial distribution of temperature (OK) in the CMIP6 models compared to the IMD temperature during 1979-2014. From this Fig., it can be seen that the IITM-ESM, CESM-2, MIROC6, and MPI-ESM-LR models fare better than the other models in terms of temperature distribution. From bias plots of temperature (Fig. 8) models, ACCESS, CESM2, GISS-E2-G, and MIROC-6 models overestimated the temperature up to 5-70C, and IITM-ESM, IPSL-CM6A-LR, and MIP models underestimated the temperature up to 30°C. All the models are underestimating the temperature in Jammu and Kashmir, some parts of the northeastern state region, up to 150°C.

The IITM ESM model shows slightly low temperatures over central India and very low temperatures over the Jammu and Kashmir regions as compared with the models. In Fig. 9, the Taylor diagram of the monthly mean temperatures of the models shows that the GISS and IITM-ESM models are close to the observation, and the IITM-ESM and Had GEM models are strongly correlated with the model. The ensemble of the models has an excellent correlation with the observation.

Precipitation in CMIP6 Models: Fig. 10 shows the spatial distribution of precipitation (mm/day) of CMIP6 models compared to the IMD precipitation during 1979-2014. From this Fig., it can be seen that the IITM, CESM, GISS, MIROC, IPSL, MIROC, and MPI models fare better than the other models in terms of rainfall distribution.

From the Bias plots (Fig. 11), CESM, HADGEM, IITM-ESM, and MPI models underestimate the precipitation up to 3-6mm/day, and ACCESS, GISS, IPSL, MIROC models are overestimating (0-3mm.day⁻¹) over the south peninsular parts of India. IITM model is slightly

overestimating in the Jammu and Kashmir regions and underestimating in the western Ghats regions.

CMIP-6 models are simulating the precipitation with low(Positive and Negative) biases, which is a good indication in modeling. Fig. 12 shows the Taylor diagram of the monthly mean precipitation of models, shows that CESM and GISS models are close to the observation but have low correlation, and IITM-ESM shows a higher correlation than all other models.

Pressure at mean sea level in CMIP6 models: The models CESM, GISS, IPSL, and MIROC are performing good simulations when compared with the observation; models IITM, HAD, ACCESS, and MPI are not performing good simulations when compared with the observation obtained from ERA.

Fig. 14 shows the Taylor diagram of monthly mean pressure at mean sea level for the models, showing that CESM, GISS, IPSL, and MIROC are close to the observation.

Wind patterns in CMIP6 models, zonal and meridional: Fig. 15 shows that the models ACCESS, HAD, and IPSL perform better simulations compared with the observation taken from the ERA reanalysis. Figs. 16a & 16b shows the Taylor diagram of U Wind AND V Wind, which shows that all the models' correlation is very low. ACCESS is close to the observation in U-Wind, and ACCESS GISS CESM MIROC MPI is very close to the observation in V-Wind.

CONCLUSION

The Indian summer monsoon was analyzed using coupled climatological models from 1979 to 2014. Data from the CMIP5 and CMIP6 model datasets, each containing seven models, were downloaded and studied. The IITM-ESM model was also compared with the CMIP-6 model. The main results showed that the CESM1 (CAM5), GISS-E2.1-G, and CMIP5 models showed low correlation values for precipitation and temperatures compared to observations.

The GISS-E2.1-G, CESM-2, and MIROC5 models showed better performance compared to the other models. The Taylor score of the ACCESS-CM-1, MIROC5, and GISS-E2.1-G models had the highest skill level, whereas the Interannual Variability Score of the MIROC5 and GISS-E2.1-G CESM-2 models had the highest IVS skill level. The IITM-ESM, CESM-2, MIROC6, and MPI-ESM-LR models outperformed the other models in terms of temperature distribution. However, the models ACCESS, CESM2, GISS-E2-G, and MIROC-6 overestimate temperatures up to 5-70 C and underestimate temperatures up to 30°C. The IITM ESM model revealed slightly low temperatures in central India and very low temperatures in the Jammu and Kashmir regions. The models performed better in simulations than in observation, with CESM, GISS, IPSL, and MIROC performing better than the IITM, HAD, ACCESS, and MPI models.

The wind patterns in the CMIP6 models were also close to the observations. We found that only a slight improvement occurred in the CMIP6 models but not substantial in the simulation of temperature and precipitation. Upon analyzing the CESM-2 model results, it was found that the model performs better simulations of temperature than the other CMIP-6 models. GISS-

E2.1-G is the model that is performing better simulations of precipitation in CMIP6 models. CESM, GISS, IPSL, and MIROC models are performing better simulations of pressure at mean sea level pressure in CMIP-6 models. ACCESS model is performing better simulations of zonal and meridional winds.

The model showed a good response to temperature and precipitation simulations, although there are slight biases that need to be enhanced. However, most studies have focused on the simulation ability of the study region and have overlooked the influence of topography on model performance. The topography of Asia is complex and significant, making it unscientific to ignore regional differences and discuss model applicability. Both equal-weight and non-equal-weight methods were used to average multi-model ensembles and analyze individual models' performance in extreme precipitation regions.

Using the CMIP 6 multi-model ensembles downscaled to the scale at which the crop and livestock would be useful for adaptation planning and investment. Crop and livestock models were run on a site-specific basis to simulate the effects of climate change on relative yield distribution in the farm population. These models can be used to evaluate how system adaptation can alter the impacts of climate change. Changes in planting dates, fertilizer application rates, and irrigation use can be modified in crop models.

REFERENCES

- Asharaf, S. and Ahrens, B., 2015. Indian summer monsoon rainfall processes in climate change scenarios. *Journal of Climate*, 28(13), pp.5414-5429
- Bollasina, M., Ming, Y. and Ramaswamy, V., 2011. Anthropogenic Aerosols and the Weakening of the South Asian Summer Monsoon. *Journal of Climate*, 24(24), pp.6031-6046.
- Bonan, G.B., 2008. Forests and climate change: Forcings, feedbacks, and the climate benefits of forests. *Science*, 320(5882), pp.1444-1449.
- Chaturvedi, R.K., Joshi, J., Jayaraman, M., Bala, G. and Ravindranath, N.H., 2012. Multi-model climate change projections for India under representative concentration pathways. *Current Science*, 103(7), pp.791-802.
- Deser, C., Alexander, M.A., Xie, S.P. and Phillips, A.S., 2010. Sea surface temperature variability: Patterns and mechanisms. *Annual Review of Marine Science*, 2(1), pp.115-143.
- Intergovernmental Panel on Climate Change (IPCC), 2021. The Physical Science Basis. ISBN 978-92-9169-158-6.
- Jin, Q. and Wang C., 2017. A revival of Indian summer monsoon rainfall since 2002. *Nature Climate Change*, 7(8), pp.587-594.
- Kannan, S. and Ghosh, S., 2013. A Nonparametric Kernel Regression Model for Downscaling Multisite Daily Precipitation in the Mahanadi Basin. *Water Resources Research*, 49, pp.1360-1385.
- Krishnan, R., 2012. Conserved features of intermediates in amyloid assembly determine their benign or toxic states. *Proceedings of the National Academy of Sciences of the United States of America*, 109(28), pp.11172-11177.
- Lee, J.Y. and Wang, B., 2014. Future change of global monsoon precipitation in the CMIP5. *Climate Dynamics*, 42(1), pp.101-119.
- Mei, W., Xie, S.-P., Primeau, F., McWilliams, J.C. and Pasquero, C., 2015. Northwestern Pacific typhoon intensity controlled by changes in ocean temperatures. *Nature Geoscience*, 8(2), pp.140-144.
- Menon, A., Levermann, A., Schewe, J., Lehmann, J. and Frieler, K., 2013. Consistent increase in Indian monsoon rainfall and its variability across CMIP-5 models. *Earth System Dynamics*, 4(2), pp.287-300.
- Mishra, V., Shah, R. and Thrasher, B., 2014. Soil moisture droughts under the retrospective and projected climate in India. *Journal of Hydrometeorology*, 15(6), pp.2267-2292.
- Mishra, V., Smoliak, B.V., Lettenmaier, D.P. and Wallace, J.M., 2012. A prominent pattern of year-to-year variability in Indian Summer Monsoon Rainfall. *Proceedings of the National Academy of Sciences of the United States of America*, 109(19), pp.7213-7217.

- Ramanathan, V., Chung, C., Kim, D., Bettge, T., Buja, L., Kiehl, J., Washington, W., Fu, Q., Sikka, D. and Wild, M., 2005. Atmospheric brown clouds: Impacts on South Asian climate and hydrological cycle. *Proceedings of the National Academy of Sciences*, 102, pp.5326–5333.
- Reuter, M., Piller, W.E., Harzhauser, M. and Kroh, A., 2013. Cyclone trends constrain monsoon variability during late Oligocene sea level high stands (Kachchh Basin, NW India). *Climate of the Past*, 9(1), pp.1–15.
- Salvi, A., 2013. High-resolution multisite daily rainfall projections in India with statistical downscaling for climate change impact assessment.
- Sharma, A., Hamlet, A.F., Fernando, H.J.S., Catlett, C.E., Horton, D.E., Kotamarthi, V.R., Kristovich, D.A.R., Packman, A.I., Tank, J.L. and Wuebbles, D.J., 2018. The need for an integrated land-lake-atmosphere modeling system, exemplified by North America's Great Lakes region. *Earth's Future*, 6(10), pp.1366-1379.
- Sharmila, S., Joseph, S., Sahai, A.K., Abhilash, S. and Chattopadhyay, R., 2015. Future projection of Indian summer monsoon variability under climate change scenario: an assessment from CMIP5 climate models. *Global and Planetary Change*, 124, pp.62–78.
- Si, S., Bi, X.Q., Kong, X.H. and Hua, W., 2020. Analysis of the spatiotemporal distribution characteristics of major greenhouse gases and aerosol emissions intensity in CMIP6 scenarios. *Climate and Environmental Research*, 25, pp.366–384.
- Song, Y.J., Li, X.F., Bao, Y., Song, Z., Wei, M., Shu, Q. and Yang, X., 2020. FIO-ESM v2.0 Outputs for the CMIP6 Global Monsoons Model Intercomparison Project Experiments. *Advances in Atmospheric Sciences*, 37, pp.1045–1056.
- Taylor, K.E., 2001. Summarizing multiple aspects of model performance in a single diagram. *Journal of geophysical research: atmospheres*, 106(D7), pp.7183-7192.
- Zhang, P., Zang, J. and Chen, M., 2016. Economic impacts of climate change on agriculture: the importance of additional climatic variables other than temperature and precipitation. *Journal of Environmental Economics and Management*, 83(4), pp.91-108.

Table 1: List of CMIP5 models used for the study.

Model ID	Institute	Country	Horizontal resolution	Temporal resolution
GISS-E2-R	The National Aeronautics and Space Administration	USA	2.50 ⁰ × 2.50 ⁰	1979-2014
MPI-ESM-LR	Max Plank Institute For Meteorology	GERMANY	2.50 ⁰ × 2.50 ⁰	1979-2014
ACCESS-1-0	CSIRO Climate Science Centre	AUSTRALIA	2.50 ⁰ × 2.50 ⁰	1979-2014
IPSL-CM5A-LR	Institute for Pierre-Simon Laplace	FRANCE	2.50 ⁰ × 2.50 ⁰	1979-2014
NCAR-CESM2	National Center for Atmospheric Research	USA	2.50 ⁰ × 2.50 ⁰	1979-2014
Had GEM-2-ES	Met Office Hadley Center	UK	2.50 ⁰ × 2.50 ⁰	1979-2014
MIROC 5	University of Tokyo, National Institute for Environmental Studies, and Japan Agency for Marine-Earth Science and Technology (MIROC)	JAPAN	2.50 ⁰ × 2.50 ⁰	1979-2014

Table 2: List of CMIP6 models used for the study.

Model ID	Institute	Country	Horizontal resolution	Temporal resolution
IITM-ESM	Indian Institute of Tropical Meteorology, Pune	INDIA	2.50 ⁰ × 2.50 ⁰	1979-2014
GISS-E2.1-G	The National Aeronautics and Space Administration	USA	2.50 ⁰ × 2.50 ⁰	1979-2014
MPI-ESM-1.2-HAM	Max Plank Institute For Meteorology	GERMANY	2.50 ⁰ × 2.50 ⁰	1979-2014
ACCESS-CM2	CSIRO Climate Science Centre	AUSTRALIA	2.50 ⁰ × 2.50 ⁰	1979-2014
IPSL-CM6A-LR	Institute for Pierre-Simon Laplace	FRANCE	2.50 ⁰ × 2.50 ⁰	1979-2014
NCAR-CESM2	National Center for Atmospheric Research	USA	2.50 ⁰ × 2.50 ⁰	1979-2014
Had GEM3-GC3.1	Met Office Hadley Center	UK	2.50 ⁰ × 2.50 ⁰	1979-2014
MIROC 6	University of Tokyo	JAPAN	2.50 ⁰ × 2.50 ⁰	1979-2014

Table 3: Table showing the skill scores of fourteen CMIP5 and CMIP6 models estimates of the monthly mean temperatures during the Indian summer monsoon.

MODEL	Taylor-score	Interannual Variability Score
ACCESS 1-0	0.3609	0.1114
CESM1-CAM5	0.2892	0.3247
ENS OF CMIP5	0.2052	3.985
GISS-E2-R	0.1442	3.539
HadGEM2-ES	0.3201	0.5404
IPSL-CM5A-LR	0.2399	1.126
MIROC-5	0.3434	0.0018

MPI-ESM-LR	0.2582	1.302
ACCESS-CM2	0.2428	1.322
CESM2-CAM6	0.3184	0.01962
ENS-CMIP5	0.2248	2.797
GISS-E2.1-G	0.338	0.04993
HadGEM3-GC3.1	0.3227	0.1932
IPSL-CM6A-LR	0.3114	0.562
MIROC-6	0.3082	0.1224
MPI-ESM-1.2-HAM	0.2453	1.203

Table 4: Table showing skill scores of fourteen model estimates of the monthly mean precipitation during Indian summer monsoon.

MODELS	TS	IVS
ACCESS-CM-1	0.3609	0.1114
CESM-1	0.2892	0.3247
ENS-CMIP5	0.2052	3.985
GISS-E2.1-G	0.1442	3.539
HAD-GEM-ES2	0.3201	0.5404
IPSL-CM5A-LR	0.2399	1.126
MIROC-5	0.3434	0.001795
MPI-ESM-1.2	0.2582	1.302
ACCESS-CM-2	0.2428	1.322
CESM-2	0.3184	0.01962
ENS-CMIP6	0.2248	2.797
GISS-E2.1	0.338	0.04993
HAD-GEM-GC3.1	0.3227	0.1932
IPSL-CM6A	0.3114	0.562
MIROC-6	0.3082	0.1224
MPI-ESM-1.2	0.2453	1.203

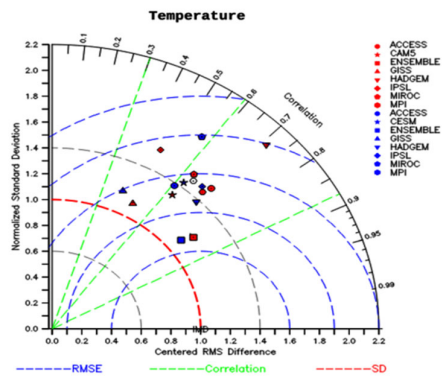


Fig. 1: Taylor diagram displaying a statistical comparison of fourteen CMIP model estimates of the monthly mean surface temperature with observations during the Indian summer monsoon.

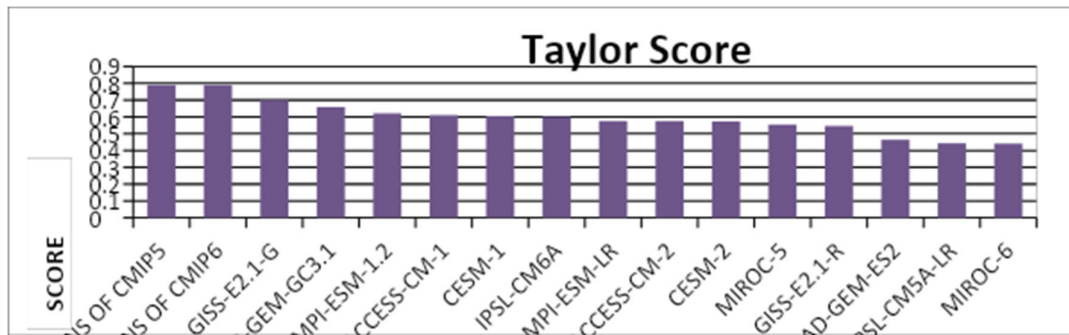


Fig. 2: Taylor score of 14 CMIP5 and CMIP6 models for monthly mean temperatures(1979-2014) compared with IMD temperature (X-axis).

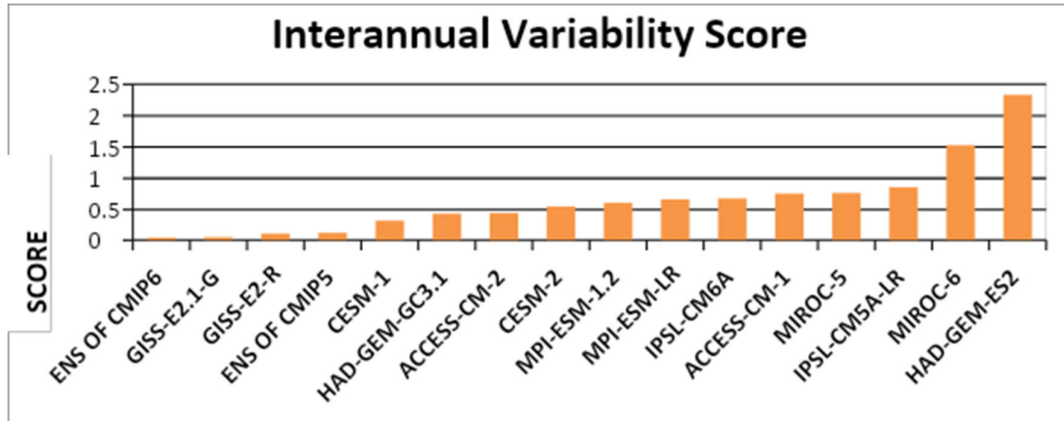


Fig. 3: Interannual variability score (IVS) of CMIP5 and CMIP6 models for monthly mean temperatures (1979-2014) compared with IMD temperature (X-axis).

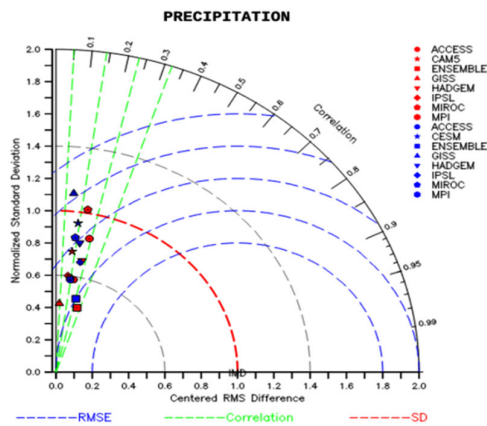


Fig. 4: Taylor diagram displaying a statistical comparison of CMIP5 and CMIP6 model estimates of the monthly mean precipitation with observations during the Indian summer monsoon.

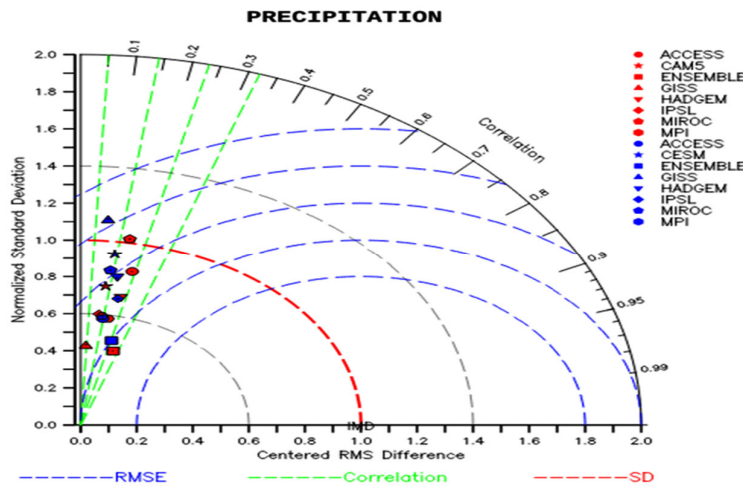


Fig. 5: Taylor scores of 14 CMIP5 and CMIP6 models for monthly mean precipitation (1979-2014) compared with IMD gridded rainfall (X-axis).

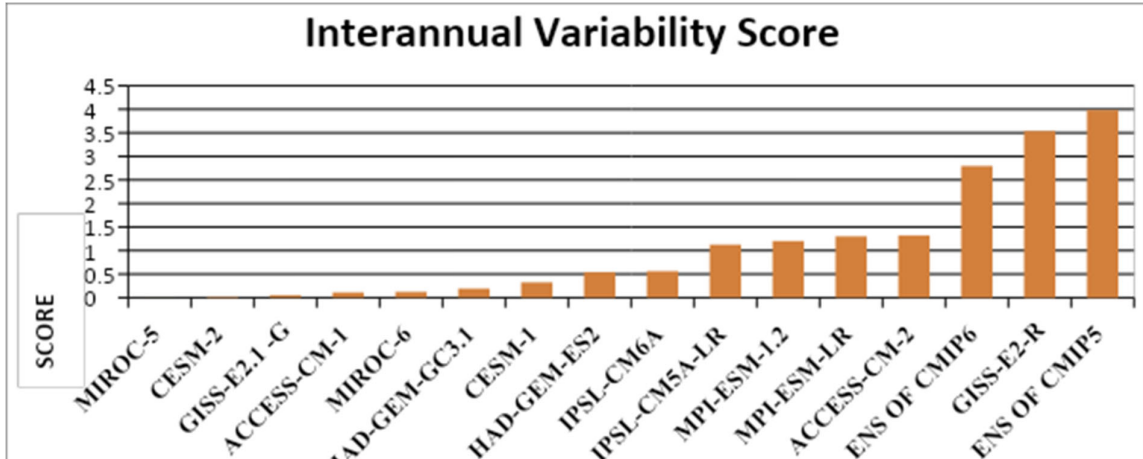


Fig. 6: Interannual variability score (IVS) of CMIP5 and CMIP6 models for monthly mean precipitation (1979-2014) compared with IMD gridded rainfall (X-axis).

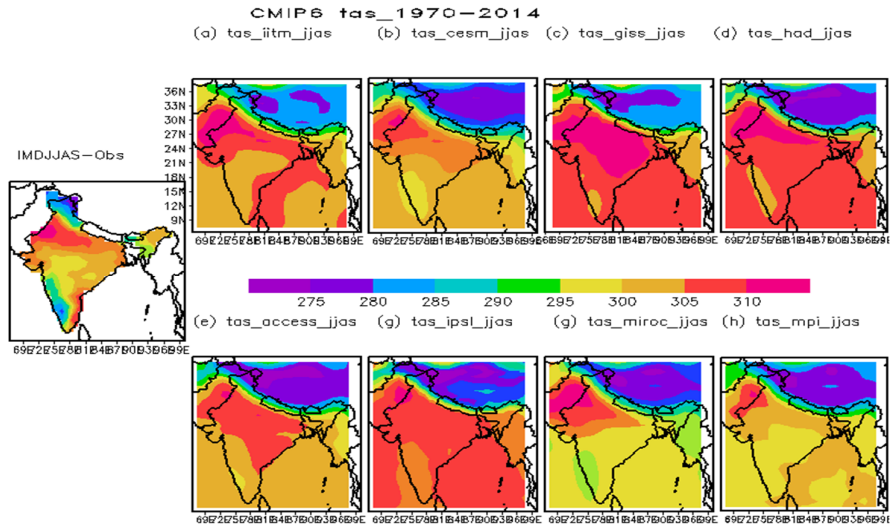
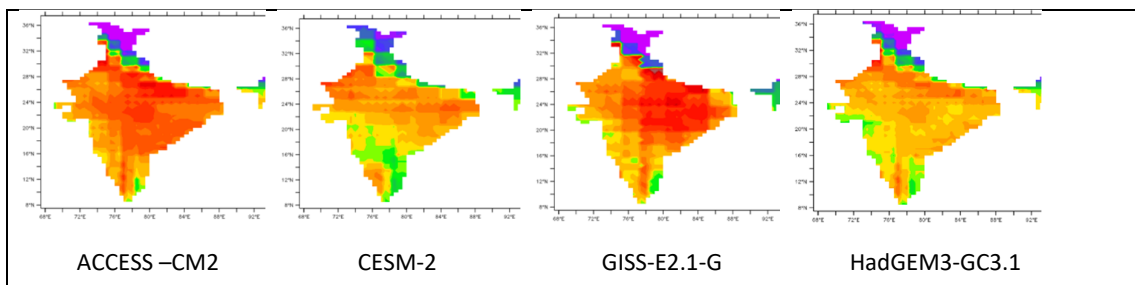


Fig. 7: Spatial distribution of temperature ($^{\circ}$ K) of 8 CMIP-6 models(a-h) compared to the IMD temperature during 1979-2014.



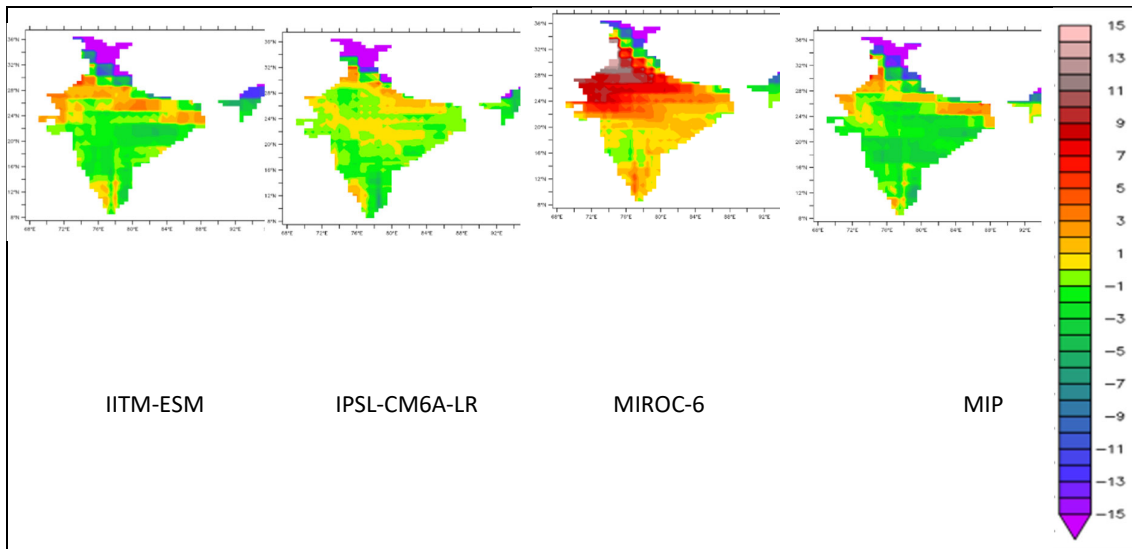


Fig. 8: Temperature biases from observation (IMD) and 8 CMIP-6 models.

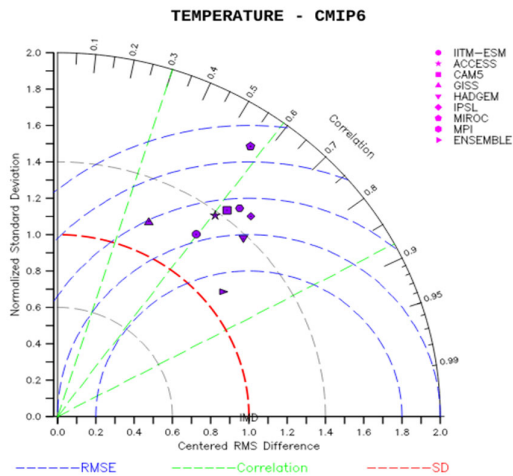


Fig. 9: Taylor diagram of monthly mean temperature variance (JJAS) for observation and 8 CMIP-6 models, the standard deviation is represented by radial distance from the origin, the correlation coefficient is represented by the azimuthal position, and the distance of the test field from observation represents centered root mean square deviation.

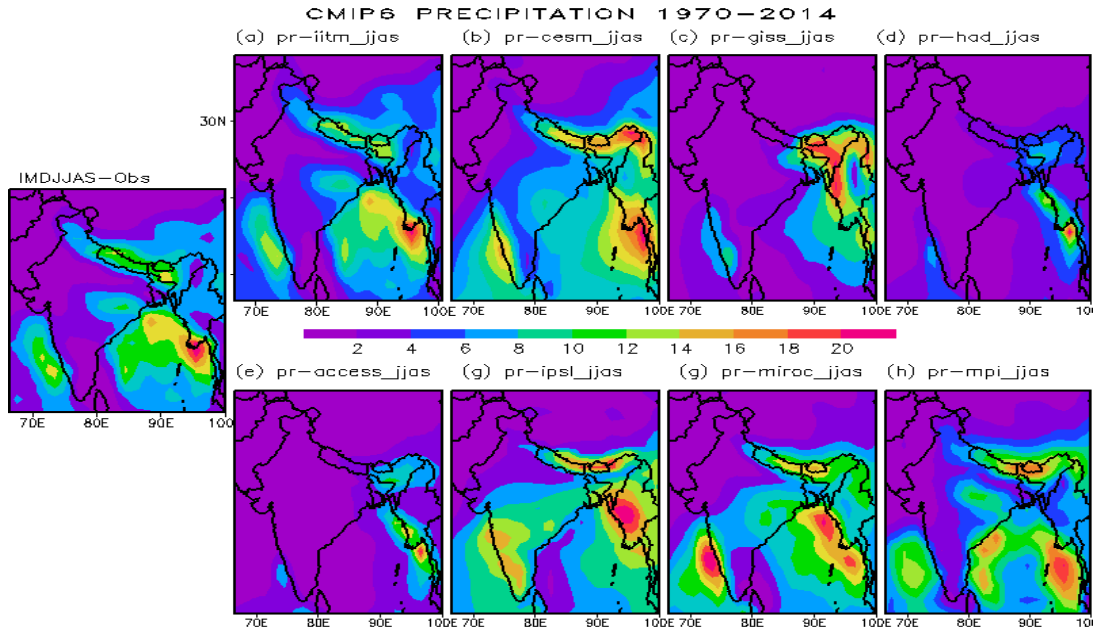


Fig. 10: Spatial distribution of precipitation of 8 CMIP-6 models(a-h) compared to the IMD precipitation during 1979-2014.

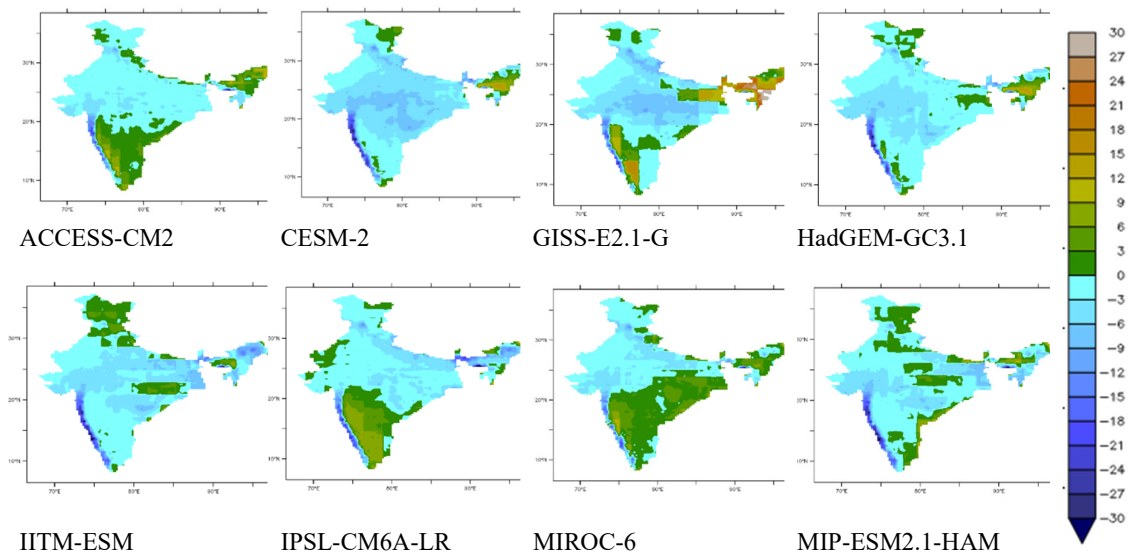


Fig. 11: Precipitation biases from observation (IMD) and 8 CMIP-6 models

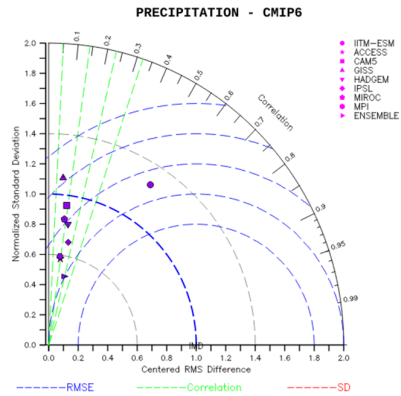


Fig. 12: Taylor diagram of monthly mean precipitation variance (JJAS) for observation(IND) and 8 CMIP-6 models, the standard deviation is represented by radial distance from the origin, the correlation coefficient is represented by the azimuthal position and distance of the test field from observation represent centered root mean square deviation.

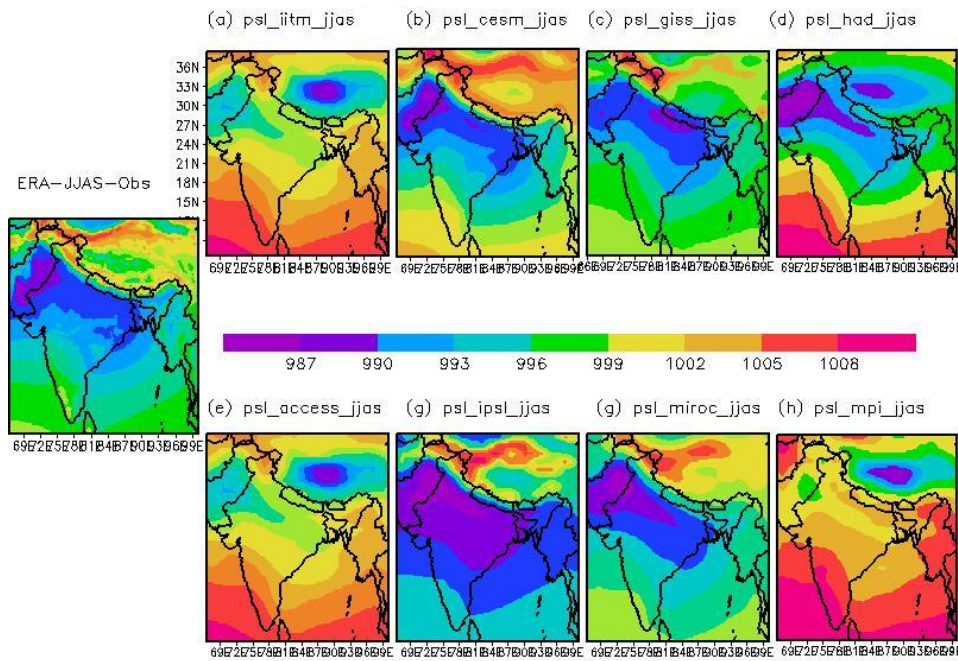


Fig. 13: Panel Plots of monthly means of pressure at mean sea level of observation and 8 CMIP-6 models (a-h).

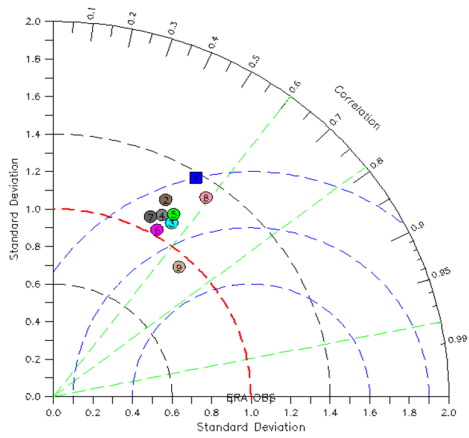


Fig. 14: Taylor diagram of monthly(JJAS)means of pressure at mean sea level (PSL) variance for observation(ERA)and 8 CMIP-6 models; standard deviation is represented by radial distance from the origin, the correlation coefficient is represented by the azimuthal position and distance of the test field from observation represent centered root mean square deviation.

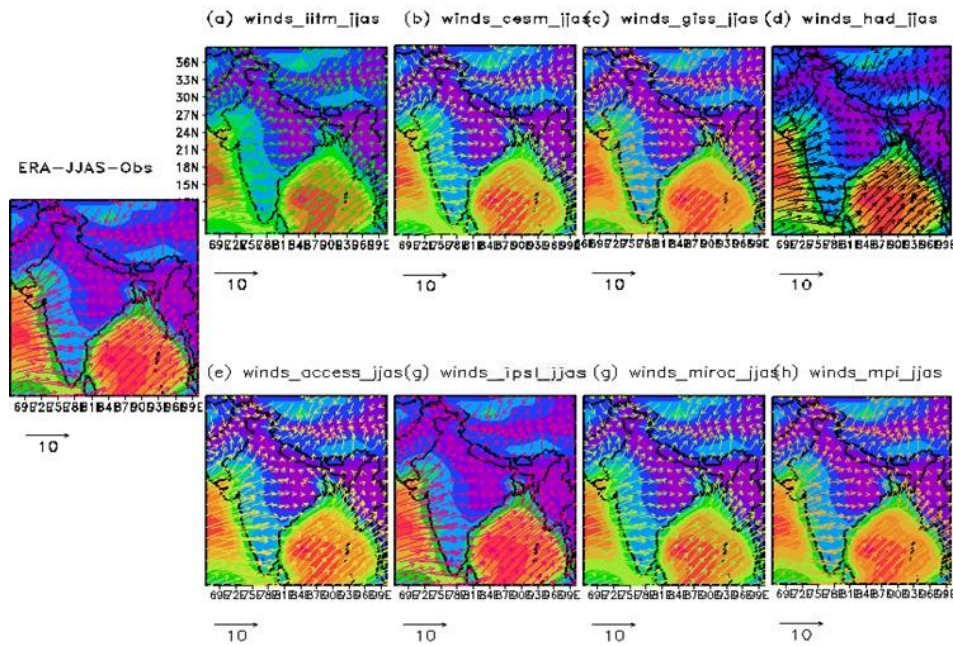


Fig. 15: Plots of Mean Zonal and Meridional winds of observation (ERA) and 8 CMIP-6 models.

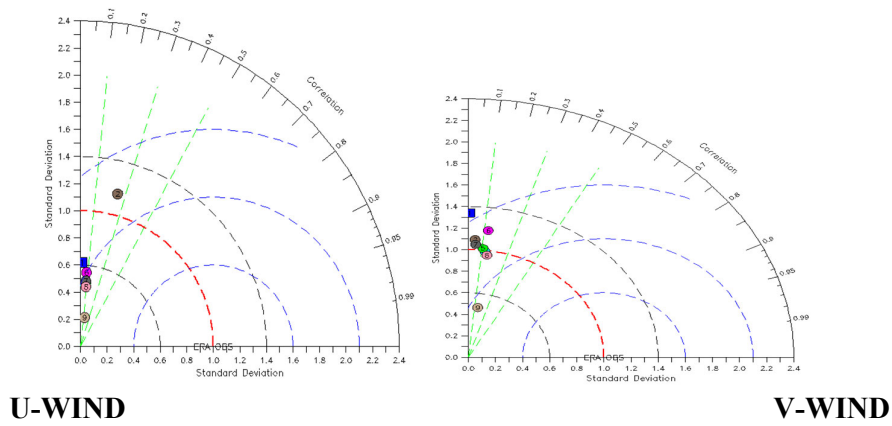


Fig. 16: Taylor diagram for a variance of (a) zonal wind and (b) meridional wind from 8 CMIP6 models.

